## • Supplementary File •

# Finite-iteration model-free adaptive terminal iterative learning control

Xuhui BU<sup>1,2</sup>, Chaohua YANG<sup>1</sup> & Yanling YIN<sup>3\*</sup>

<sup>1</sup>School of Electrical Engineering and Automation, Henan Polytechnic University, Jiaozuo 454003, China <sup>2</sup>Henan Key Laboratory of Intelligent Detection and Control of Coal Mine Equipment, Henan Polytechnic University, Jiaozuo 454003, China

 $^3$ School of Business Administration, Henan Polytechnic University, Jiaozuo 454003, China

**Lemma 1.** If  $0 < \sigma < 1$  and function  $p(\sigma) = 1 + \sigma^{\frac{\sigma}{1-\sigma}} - \sigma^{\frac{1}{1-\sigma}}$  then  $xp(\sigma) - x^{\sigma}p^{\sigma}(\sigma) + p(\sigma) - 1 \ge 0$  for any  $x \in [0,1]$ 

Proof.

First, denote  $Q(x) = xp(\sigma) - x^{\sigma}p^{\sigma}(\sigma) + p(\sigma) - 1$ . Next, it is only necessary to demonstrate that the minimum value of Q(x) is greater than zero when  $x \in [0,1]$ . According to the figure 1, it is clear that  $1 < p(\sigma) < 2$ , then we can get that  $Q(0) = p(\sigma) - 1 > 0$  and  $Q(1) = p(\sigma) - p^{\sigma}(\sigma) + p(\sigma) - 1 > 0$ . Secondly, by taking the derivative of Q, one obtains  $\dot{Q}(x) = p(\sigma) - \sigma x^{\sigma-1}p^{\sigma}(\sigma)$ . It is clear that  $\dot{Q}(x) > 0$  when  $x \in [0,1]$ , therefore Q(x) is a monotonically increasing function. Then, we obtain that  $\min_{x \in [0,1]} Q(x) = Q(0) = 0$ , which completes the proof.

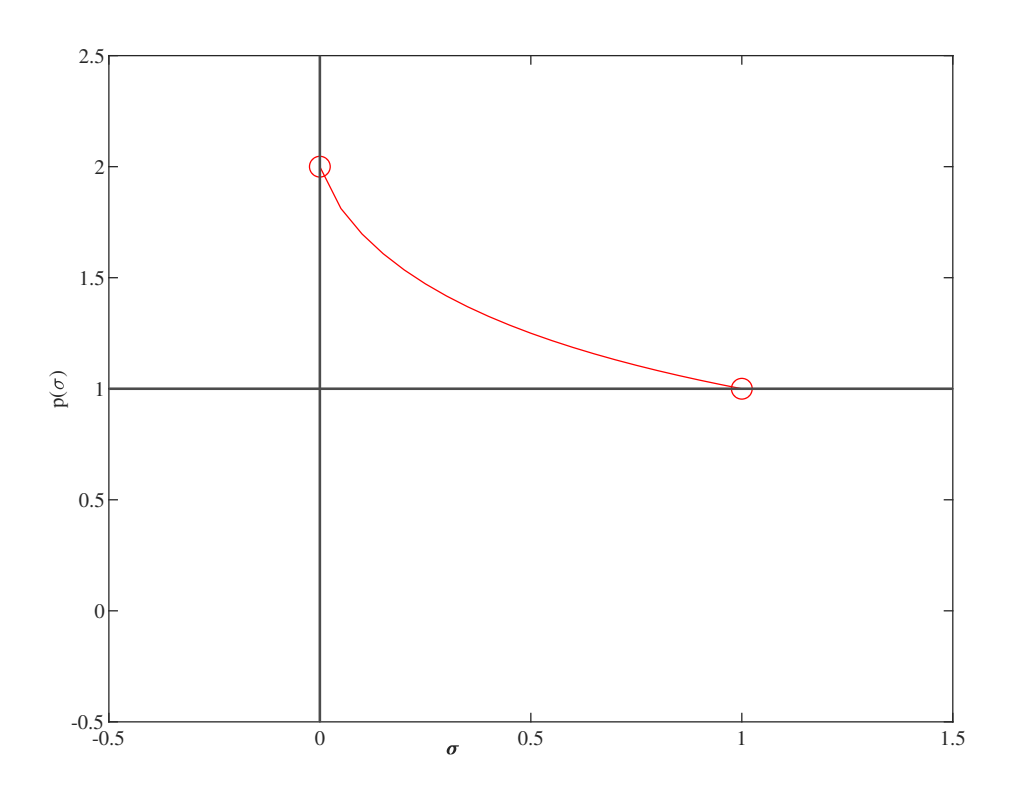


**Figure 1** Plot of function  $p(\sigma)$ .

 $<sup>\</sup>hbox{$^*$ Corresponding author (email: yinyl@hpu.edu.cn)}\\$ 

### Appendix A Proof of Theorem 1

Proof. First, define  $\mho_2 = \left\{ |h_k(t)| \leqslant p(\sigma) \cdot \max\left( (\lambda/a)^{\frac{1}{\sigma}}, \left( \frac{a}{1-b} \right)^{\frac{1}{1-\sigma}} \right) \right\}$ , where  $p(\sigma) = 1 + \sigma^{\frac{\sigma}{1-\sigma}} - \sigma^{\frac{1}{1-\sigma}}$ . The following proof can be divided into two steps. The first step is to demonstrate that  $h_k(t)$  can enter the bounded region  $\mho_2$  within finite-iteration. The second step is to ensure that  $h_k(t)$  does not leave the bounded region  $\mho_2$  after entering it.

Step 1: Considering Lyapunov function  $V_k(t) = h_k^2(t)$ , according to equation (5) that

$$\Delta V_k(t) = V_{k+1} - V_k(t) = -\left(ah_k^{\sigma}(t) + bh_k(t) - O_k(t)\right) \left(2h_k(t) - ah_k^{\sigma}(t) - bh_k(t) + O_k(t)\right). \tag{A1}$$

Next, our target is to prove that  $\Delta V_k(t) < -c$  when  $h_k(t) \notin \mathcal{O}_2$ , where c is a small positive constant. If  $h_k(t)$  is not in the bounded region  $\mathcal{O}_2$ , there are two cases for  $h_k(t)$ .

Case 1: 
$$h_k(t) > p(\sigma) \cdot \max\left( (\lambda/a)^{1/\sigma}, \left( \frac{a}{1-b} \right)^{\frac{1}{1-\sigma}} \right)$$
.

For one thing, if  $(\lambda/a)^{1/\sigma} > \left(\frac{a}{1-b}\right)^{\frac{1}{1-\sigma}}$ , we can obtain  $h_k(t) > p(\sigma)(\lambda/a)^{1/\sigma}$ , then  $ah_k^{\sigma}(t) > p^{\sigma}(\sigma)\lambda$ . By noticing that  $|O_k(t)| < \lambda$ , we have

$$ah_k^{\sigma}(t) - |O_k(t)| + bh_k > (p^{\sigma}(\sigma) - 1)\lambda + bh_k := \vartheta. \tag{A2}$$

Since  $p(\sigma) \in (1,2)$ ,  $\lambda > 0$ , then  $\vartheta > 0$ . For another thing, if  $(\lambda/a)^{1/\sigma} < \left(\frac{a}{1-b}\right)^{\frac{1}{1-\sigma}}$ , we can obtain  $h_k(t) > p(\sigma)\left(\frac{a}{1-b}\right)^{\frac{1}{1-\sigma}}$ , then  $h_k^{1-\sigma}(t) > p^{1-\sigma}(\sigma)\left(\frac{a}{1-b}\right)$ , further obtain  $(1-b)h_k(t) > p^{1-\sigma}(\sigma)ah_k^{\sigma}(t) \geqslant ah_k^{\sigma}(t)$ . Based on this inequality and (A2),  $2h_k(t) - ah_k^{\sigma}(t) - bh_k(t) + O_k(t) > ah_k^{\sigma}(t) + O_k(t) + bh_k(t) > \vartheta$  is given. Substituting this inequality and (A2) into (A1) gives  $\Delta V_k(t) < -\vartheta^2 := -c$ .

Case 2: 
$$h_k(t) \leq -p(\sigma) \cdot \max\left(\left(\lambda/a\right)^{1/\sigma}, \left(\frac{a}{1-b}\right)^{\frac{1}{1-\sigma}}\right)$$
.

If  $(\lambda/a)^{1/\sigma} > \left(\frac{a}{1-b}\right)^{\frac{1}{1-\sigma}}$ , we get  $h_k(t) \leqslant -p(\sigma)(\lambda/a)^{1/\sigma}$ , then  $ah_k^{\sigma}(t) \leqslant -p^{\sigma}(\sigma)\lambda$ , further we obtain

$$ah_k^{\sigma}(t) + bh_k - O_k(t) \leqslant (-p^{\sigma}(\sigma) + 1)\lambda + bh_k := \nu. \tag{A3}$$

where  $\nu$  is a negative number since  $p^{\sigma}(\sigma) > 1$  and  $\lambda > 0$ . On the other hand,  $h_k(t) \leqslant -p(\sigma) \left(\frac{a}{1-b}\right)^{\frac{1}{1-\sigma}}$ , then  $(1-b)(-h(t))_k^{1-\sigma} \geqslant p^{1-\sigma}(\sigma)a$ , which implies  $(1-b)h_k(t) \leqslant p^{1-\sigma}(\sigma)ah_k^{\sigma}(t)$ . It follows from this inequality and A3, we can get

$$2h_k(t) - ah_k^{\sigma}(t) - bh_k + O_k(t) \le (2p^{1-\sigma}(\sigma) - 1)ah_k^{\sigma}(t) + bh_k + \lambda \le ah_k^{\sigma}(t) + bh_k + \lambda \le (-p^{\sigma}(\sigma) + 1)\lambda := \nu. \tag{A4}$$

Substituting this inequality and A3 into A1 results in  $V_k(t) < -\nu^2$ . Therefore, by combining case 1 and case 2, it is guaranteed that  $h_k(t)$  enters the bounded region  $\mathfrak{V}_2$  within finite-iteration.

Step 2: In this step, we will prove that if  $h_k(t)$  is in the region  $\mathcal{O}_2$ ,  $h_{k+1}(t)$  is also in the region  $\mathcal{O}_2$ . There are also two cases that need to be discussed.

cases that need to be discussed. 
$$case1: \left(\frac{a}{1-b}\right)^{\frac{1}{1-\sigma}} \geqslant \left(\frac{\lambda}{a}\right)^{\frac{1}{\sigma}}, \text{ furthermore } \lambda \leqslant a\left(\frac{a}{1-b}\right)^{\frac{\sigma}{1-\sigma}}$$

In this case, we assume that  $h_k(t) = p(\sigma)w\left(\frac{a}{1-b}\right)^{\frac{1}{1-\sigma}}$ , 0 < w < 1. According to (5) yields

$$h_{k+1}(t) \leq (1-b)p(\sigma)w\left(\frac{a}{1-b}\right)^{\frac{1}{1-\sigma}} - a\left(p(\sigma)w\right)^{\sigma} \left(\frac{a}{1-b}\right)^{\frac{\sigma}{1-\sigma}} + \lambda$$

$$\leq (1-b)p(\sigma)w\left(\frac{a}{1-b}\right)^{\frac{1}{1-\sigma}} - a\left(p(\sigma)w\right)^{\sigma} \left(\frac{a}{1-b}\right)^{\frac{\sigma}{1-\sigma}} + a\left(\frac{a}{1-b}\right)^{\frac{\sigma}{1-\sigma}}$$

$$\leq (1-b)\left(\frac{a}{1-b}\right)^{\frac{1}{1-\sigma}} \left(p(\sigma)w + 1 - (p(\sigma)w)^{a}\right). \tag{A5}$$

Next, we discuss the cases of  $0 \le p(\sigma)w \le 1$  and  $1 \le p(\sigma)w$ , respectively. When  $0 \le p(\sigma)w \le 1$ , we can get  $(p(\sigma)w+1-(p(\sigma)w)^a) \le 1$ . In the light of this information, it follows from (A5) that  $h_{k+1}(t) \le (1-b)\left(\frac{a}{1-b}\right)^{\frac{1}{1-\sigma}} \le p(\sigma)w\left(\frac{a}{1-b}\right)^{\frac{1}{1-\sigma}}$ . If  $p(\sigma)w > 1$ , there is  $(p(\sigma)w+1-(p(\sigma)w)^\sigma) < p(\sigma)w$ , then  $h_{k+1}(t) \le p(\sigma)w\left(\frac{a}{1-b}\right)^{\frac{1}{1-\sigma}}$ .

As a result,  $h_{k+1}(t) \in \mathcal{V}_2$ . A similar proof will show that the assumption of  $h_k(t) = p(\sigma)w\left(\frac{a}{1-b}\right)^{\frac{1}{1-\sigma}}$ , -1 < w < 0, will also lead to the conclusion that  $h_{k+1}(t) \in \mathcal{V}_2$ .

 $case2: \left(\frac{\lambda}{a}\right)^{\frac{1}{\sigma}} > \left(\frac{a}{1-b}\right)^{\frac{1}{1-\sigma}}$ . Similar to the proof of Case 1, we can obtain that  $h_{k+1}(t) \in \mathcal{O}_2$ . The proof of Theorem 1 is completed here.

Remark 1. Although the proof of Theorem 1 is the same as Lemma 2 in reference [1] in terms of logical structure, the two are fundamentally different in terms of the specific dimensions of the application. Specifically, Theorem 1 is based on the iteration axis, with a focus on the dynamic behavior and stability properties of the algorithm during the iteration process. This is fundamentally different from the traditional timeline analysis. Furthermore, to deal with this two-dimensional dynamic behavior, we introduce a more complex Lyapunov function in the proof. This Lyapunov function considers the coupling effect of both time and iteration dimensions, which does not occur in analyses with a single time dimension. Thus, although seemingly similar in surface structure, our method and results demonstrate new theoretical and technical contributions in dealing with multidimensional dynamical systems.

#### Appendix B Proof of Theorem 2

*Proof.* The proof process is divided into two parts.

(I). The boundedness of estimation value  $\widehat{\Phi}_k$ 

Let  $\widetilde{\Phi}_k = \Phi_k - \widehat{\Phi}_k$  indicates the estimation error. Subtracting  $\Phi_k$  from both sides of equation (8), we have

$$\widetilde{\Phi}_{k} = \widetilde{\Phi}_{k-1} - \frac{\eta \widetilde{\Phi}_{k-1} \Delta u_{k-1} \Delta u_{k-1}}{\mu + |\Delta u_{k-1}|^{2}} + \Phi_{k} - \Phi_{k-1}. \tag{B1}$$

According to Assumption 4,  $0 < |\Phi_k| \le l_2$ , so we can easily get  $|\Phi_k - \Phi_{k-1}| < 2l_2$ . Moreover, there have  $0 < p_1 < 1$  such that the inequation  $\left(1 - \frac{\eta \Delta u_{k-1}^2}{\mu + |\Delta u_{k-1}|^2}\right) \le p_1$  holds. Furthermore, taking absolute values on both sides of (B1), one obtains

$$\left|\widetilde{\Phi}_{k}\right| \leqslant \left|\widetilde{\Phi}_{k-1} - \frac{\eta \widetilde{\Phi}_{k}^{i} \Delta u_{k-1}^{2}}{\mu + \left|\Delta u_{k-1}\right|^{2}}\right| + \left|\Phi_{k} - \Phi_{k-1}\right| \leqslant p_{1} \left|\widetilde{\Phi}_{k-1}\right| + 2l_{2}$$

$$\leqslant p_{1} \left(p_{1} \left|\widetilde{\Phi}_{k-2}\right| + 2l_{2}\right) + 2l_{2} \leqslant \cdots \leqslant p_{1}^{k} \left|\widetilde{\Phi}_{0}\right| + \frac{2l_{2}(1 - p_{1}^{k})}{1 - p_{1}}.$$
(B2)

which means that  $\widetilde{\Phi}_k$  is bounded. Then, according to  $\widetilde{\Phi}_k = \Phi_k - \widehat{\Phi}_k$  and  $0 < |\Phi_k| \le l_2$ , it can be concluded that  $\widehat{\Phi}_k$  is also bounded.

(II). The terminal tracking error finite-iteration convergence property

According to (4) and (9), the terminal tracking error can be expressed as follows

$$e_k(T) = e_{k-1}(T) - \frac{2\rho\Phi\widehat{\Phi}_k}{\lambda + 4\left|\widehat{\Phi}_k\right|^2} \left(e_{k-1}^{\sigma}(T) + e_{k-1}(T)\right) = e_{k-1}(T) - \Gamma_k e_{k-1}^{\sigma}(T) - \Gamma_k e_{k-1}(T).$$
 (B3)

where  $\Gamma_k = \frac{2\rho\Phi H_k\widehat{\Phi}_k}{\lambda+4|\widehat{\Phi}_k|^2}$ . It has been demonstrated that  $\widehat{\Phi}_k$  and  $\Phi_k$  are bounded. So,  $0<|\Gamma|\leqslant \mathfrak{w}<1$  can be guaranteed under the condition of  $\lambda>\lambda_{min}$  and  $\rho<\rho_{max}$ . Therefore, according to Theorem 1, there is a finite-iteration  $k^*$ , for every iteration k such that

$$e_k(T) \leqslant \left(\frac{\mathfrak{w}}{1-\mathfrak{w}}\right)^{\frac{1}{1-\sigma}} \left(1 + \sigma^{\frac{\sigma}{1-\sigma}} - \sigma^{\frac{1}{1-\sigma}}\right) \quad \forall k > k^*.$$

which implies that  $e_k$  can converge to a bounded range within finite-iteration.

Since the tracking error  $e_k(T)$  has a finite-iterative convergence property outside the stable region, it satisfies

$$|e_k^{\sigma}(T)| \leqslant \varpi \left| e_{k-1}^{\sigma}(T) \right| \qquad 0 < \varpi \leqslant 1.$$
 (B4)

(III). The boundedness of  $u_k$ 

In order to prove  $u_k$  is bounded, we rewrite equation (9) as follows

$$\Delta u_k = \frac{2\rho \widehat{\Phi}_k}{\lambda + 4\left|\widehat{\Phi}_k\right|^2} \left(e_{k-1}^{\sigma}(T) + e_{k-1}(T)\right). \tag{B5}$$

Since  $\widehat{\Phi}_k$  is bounded, then  $\frac{2\rho\widehat{\Phi}_k}{\lambda+4|\widehat{\Phi}_k|^2}$  is also bounded. Without loss of generality, let's assume that  $\frac{2\rho\widehat{\Phi}_k}{\lambda+4|\widehat{\Phi}_k|^2} \leqslant \psi_2$  with  $\psi_2$  being a positive constant. Thus, from equation (B4) and (B5), we can eventually get

$$|u_{k}| \leq |\Delta u_{k}| + |\Delta u_{k-1}| \cdots + |u_{1}| \leq \psi_{2} \left\{ \varpi^{k-2} \left( \left| e_{1}^{\sigma}(T) \right| + |e_{1}(T)| \right) + \varpi^{k-3} \left( \left| e_{1}^{\sigma}(T) \right| + |e_{1}(T)| \right) + \cdots \right.$$

$$\left. + \left. \varpi \left( \left| e_{1}^{\sigma}(T) \right| + |e_{1}(T)| \right) + |u_{1}| \right\} \leq \frac{\psi_{2} \varpi (1 - \varpi^{k-2}) \left( \left| e_{1}^{\sigma}(T) \right| + |e_{1}(T)| \right)}{1 - \varpi} + |u_{1}|.$$
(B6)

which implies that  $u_k$  is also bounded.

#### Appendix C Simulation examples

This section presents two illustrative examples that demonstrate the efficacy of the proposed FITILC method.

Example 1. Consider a linear SISO system as follows

$$\begin{aligned} \boldsymbol{x}_k(t+1) &= \begin{pmatrix} 0.5 & 0.035 & 0.025 \\ 0.0255 & 0.6 & -0.99 \\ 0.75 & 0.03 & 0.025 \end{pmatrix} \boldsymbol{x}_k(t) + \begin{pmatrix} 0.2 & 0.2 & 0.0 \end{pmatrix}^T u_k(t) \\ y(t) &= \begin{pmatrix} 1.0 & 0.0 & 1.0 \end{pmatrix}^T \boldsymbol{x}_k(t) \end{aligned}$$

where  $t \in \{0, \dots 20\}$ , desired terminal trajectories  $y_d(20) = 2$ .

In the simulation, the initial iteration of the control input is designated as  $u_0=0$  and the initial states are assumed as  $\boldsymbol{x}_k(0)=\begin{bmatrix}0&0&0\end{bmatrix}^T$  for every iteration k. Please note that setting the initial state and control input of the system to zero is a common and simple choice. Although the initial state theoretically affects the system's instantaneous dynamics, our focus is on the control performance of the terminal state, and this impact is designed to diminish gradually during the iteration process. In addition, the asymptotic convergence of the proposed scheme can be guaranteed by arbitrary initial input. However, choosing a suitable initial input can expedite the transient convergence rate. The initial estimation is chosen as  $\hat{\Phi}_0=1$ . Then, according to the convergence condition in Theorem 2, select the controller parameter as  $\rho=1$ ,  $\eta=0.2$ ,  $\lambda=1$ ,  $\mu=1$  and  $\sigma=7/9$ . In order to demonstrate the superiority of the method proposed in this paper, we specifically selected the control schemes from references [2] and [3] for a comparative simulation analysis with the scheme designed in this paper.

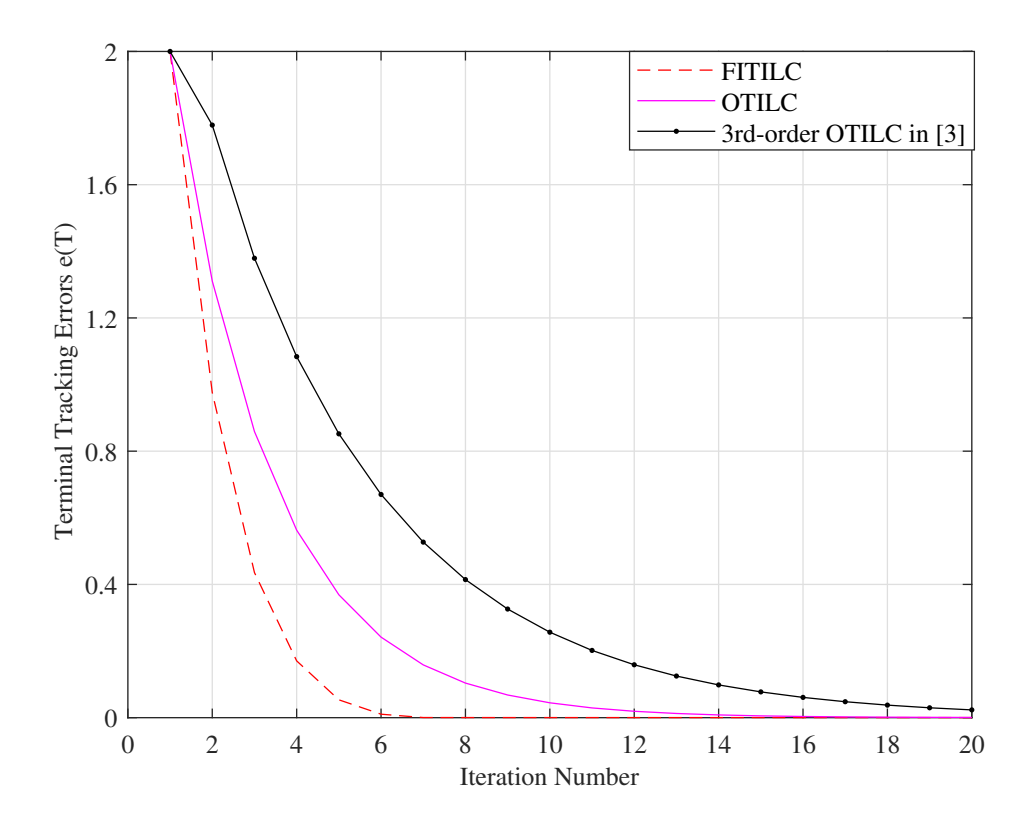


Figure C1 Terminal tracking error profile along with iteration axis.

Figure C1 shows the curve of the terminal tracking error with iteration. The horizontal axis represents the iteration number, while the vertical axis denotes the absolute value of the terminal tracking error. It is evident that the aforementioned three algorithms are capable of guaranteeing the iterative convergence of the terminal tracking error. Moreover, the tracking performance of the proposed FITILC is superior to that of OTILC, while the tracking performance of FITILC is superior to that of literature [2,3].

Control input  $u_k$  is shown in Figure C2. It is obvious that the control input is bounded. In addition, the control inputs of FITILC can reach the desired value at a faster rate than the scheme in [2,3].

**Example 2.** In order to further illustrate the applicability of the proposed approach in practical processes. A simulation is performed on realistic mechanical systems. The dynamic of systems is described as follows [4]

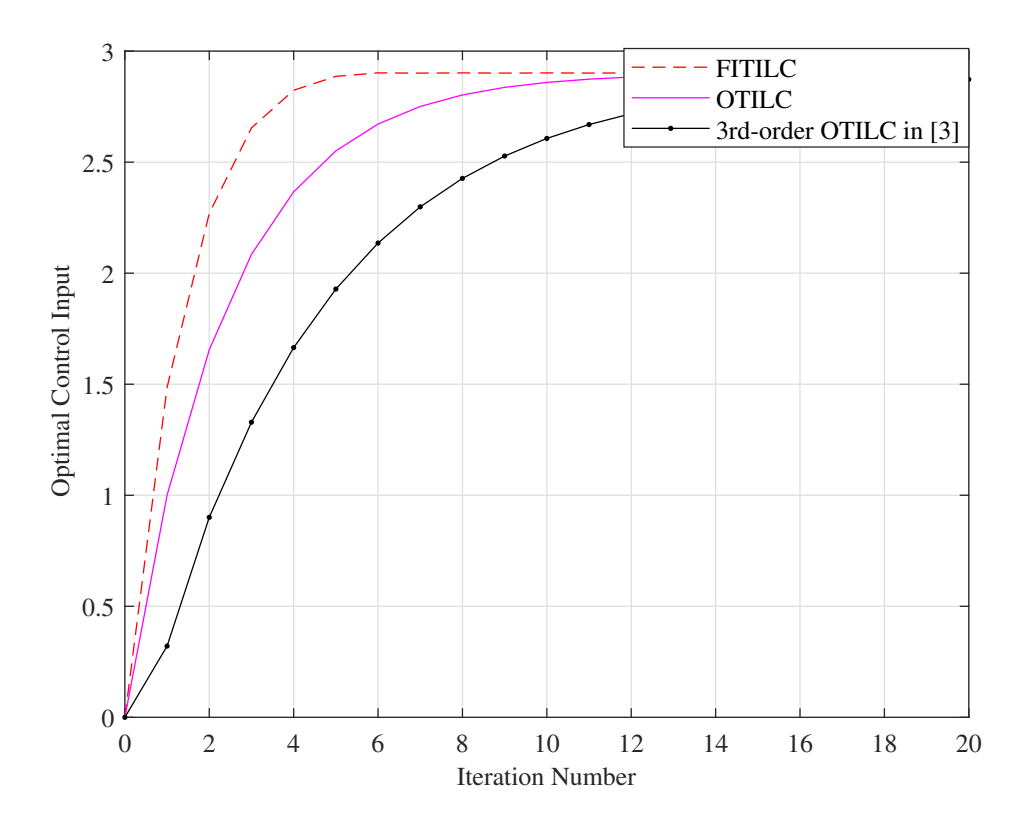


Figure C2 Optimal Control input along with iteration axis.

$$\begin{cases} \dot{x}(t) = v(t) \\ \dot{v}(t) = \frac{u(t) - f_{rip.}(t) - f_{fri.}(t)}{m} \end{cases}$$

where x(t) is position (m), v(t) is the speed (m/s), control input u(t) is the developed force (N), m is the combined mass of the translator and load,  $f_{fri.}(t) = \left(f_c + (f_s - f_c) \exp\left(-\dot{x}/\dot{x}_\delta\right)^\delta + f_v\dot{x}\right) sgn(\dot{x})$  is the friction force (N),  $f_{rip.}(t) = b_1 sin(\omega_0 x(t))$  is the ripple force (N). The parameters in the simulation are selected as: m = 0.59,  $x_\delta = 0.1$ ,  $\delta = 1$ ,  $f_c = 10$  N,  $f_s = 20$  N,  $f_v = 10$  N·s·m<sup>-1</sup>,  $\omega_0 = 314$  s<sup>-1</sup>.

Denote  $x_1(t) = x(t)$ ,  $x_2(t) = v(t)$ . Next, discretization of the above system using the forward Euler method, we can obtain

$$\begin{cases} x_1(t+1) = h \cdot x_2(t) + x_1(t) \\ x_2(t+1) = x_2(t) + \frac{h}{m} \left( u(t) - f_{rip.}(t) - f_{fri.}(t) \right) \\ y(t) = x_2(t) \end{cases}$$

where the asympling time h = 0.001,  $t \in \{0, \dots 500\}$ , terminal desired velocity is  $y_d(T) = 3$  (m/s).

The initial conditions of the system are selected as  $x_1(0) = x_2(0) = 0$ , control input u(0) = 0 for all iteration. The initial estimation is chosen as  $\widehat{\Phi}_0 = 1$ . Then, according to the convergence condition in Theorem 2, select the controller parameter as  $\rho = 1, \eta = 0.2, \lambda = 1, \mu = 1$  and  $\sigma = 7/9$ . The simulation results shown in Figure C3 show that all schemes can achieve satisfactory control performance. In addition, the FITILC achieves much better control performance compared to the existing TILC.

In practical applications, the system will be affected by various disturbances. To further demonstrate the applicability of the proposed approach to practical processes, some state disturbances and output noises are introduced to the mechanical model, shown as follows:

$$\begin{cases} x_1(t+1) = h \cdot x_2(t) + x_1(t) + w_1(t) \\ x_2(t+1) = x_2(t) + \frac{h}{m} \left( u(t) - f_{rip.}(t) - f_{fri.}(t) \right) + w_2(t) \\ y(t) = x_2(t) + n(t) \end{cases}$$

where  $w_1(t) = 0.01 \sin(t\pi/300) + 0.01 rand(1)$  and  $w_2(t) = 0.01 \sin(t\pi/600) + 0.01 rand(1)$  are the state disturbances; we let  $n(t) = 0.05 \sin(t\pi/1500) + 0.01 rand(1)$  denotes the output noise. The simulation result is shown in Figure C4. Apparently,

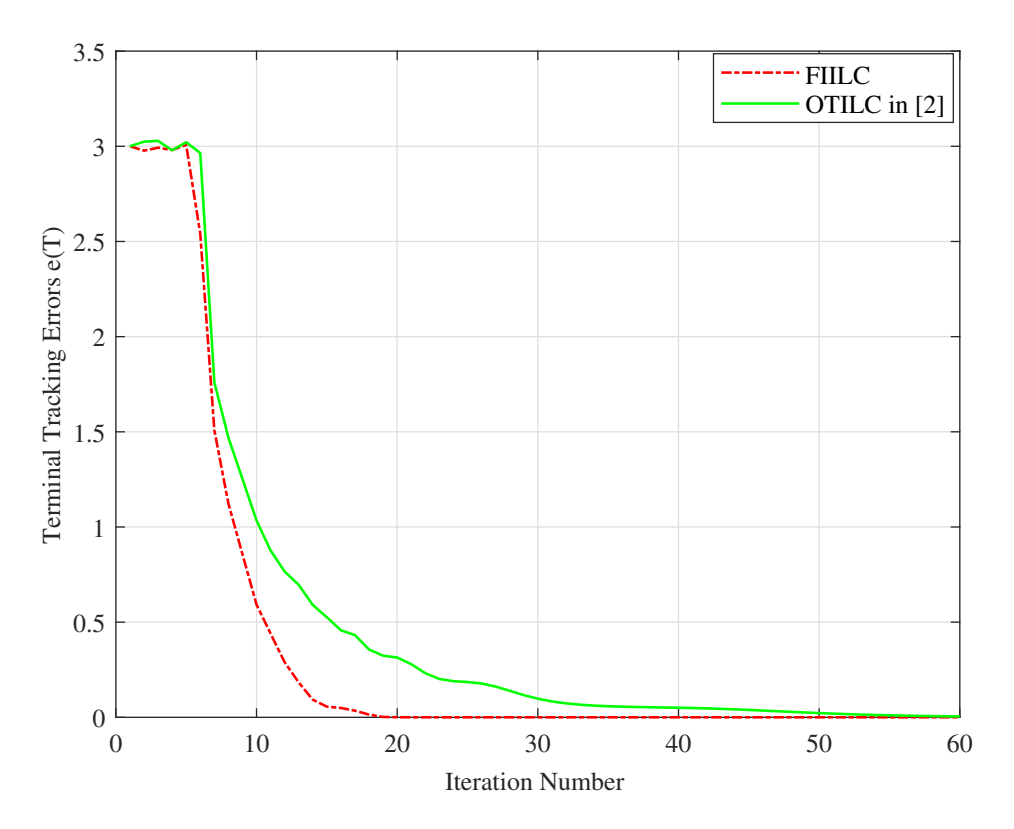


Figure C3 Terminal tracking error profile along with iteration axis.

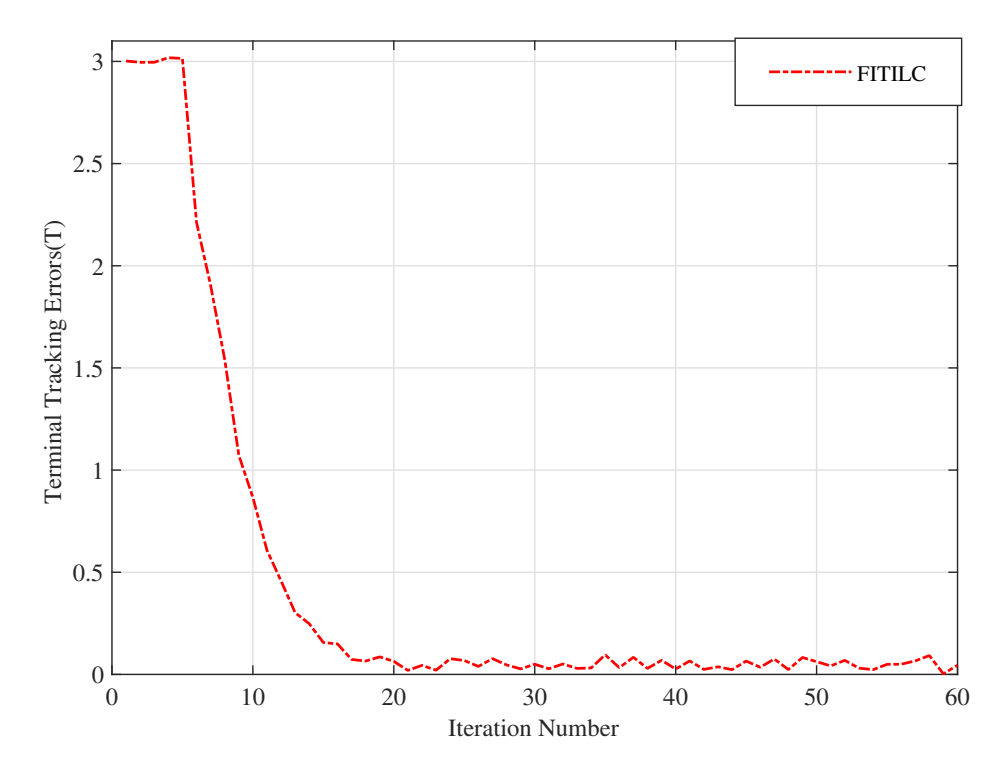


Figure C4 Terminal tracking error profile with disturbances.

the proposed approach is robust for the uncertain disturbances that exist in system states and outputs. However, there exist some deviations in output curves that are caused by stochastic measurement noises. The deviations cannot be canceled since the noise is completely unpredictable.

#### References

- 1 Li S H, Du H B, Yu X H. Discrete-Time Terminal Sliding Mode Control Systems Based on Euler's Discretization. IEEE T Automat Contr, 2014, 59:546–52
- 2 Chi R H, Wang D W, Hou Z S, et al. Data-driven optimal terminal iterative learning control. J Process Contr, 2012, 22:2026–37
- 3 Chi R H, Huang B, Hou Z S, et al. Data-driven high-order terminal iterative learning control with a faster convergence speed. Int J Robust Nonlin, 2018, 28:103–19
- 4 Bu X H, Hou Z S, Zhang H W. Data-Driven Multiagent Systems Consensus Tracking Using Model Free Adaptive Control. IEEE Trans Neural Networks Learn Syst, 2018, 29:1514–24